

Fast Multirate Encoding for 360° Video in OMAF Streaming Workflows

Amritha Premkumar, Christian Herglotz

Chair of Computer Engineering

Brandenburg University of Technology Cottbus-Senftenberg
Cottbus, Germany

ABSTRACT

Preparing high-quality 360° video for HTTP Adaptive Streaming requires encoding each sequence into multiple representations spanning different resolutions and quantization parameters (QPs). For ultra-high-resolution immersive content such as 8K 360° video, this process is computationally intensive due to the large number of representations and the high complexity of modern codecs. This paper investigates fast multirate encoding strategies that reduce encoding time by reusing encoder analysis information across QPs and resolutions. We evaluate two cross-resolution information-reuse pipelines that differ in how reference encodes propagate across resolutions: (i) a strict HD → 4K → 8K cascade with scaled analysis reuse, and (ii) a resolution-anchored scheme that initializes each resolution with its own highest-bitrate reference before guiding dependent encodes. In addition to evaluating these pipelines on standard equirectangular projection content, we also apply the same two pipelines to cubemap-projection (CMP) tiling, where each 360° frame is partitioned into independently encoded tiles. CMP introduces substantial parallelism, while still benefiting from the proposed multirate analysis-reuse strategies. Experimental results using the SJTU 8K 360° dataset show that hierarchical analysis reuse significantly accelerates HEVC encoding with minimal rate-distortion impact across both equirectangular and CMP-tiled content, yielding encoding-time reductions of roughly 33%–59% for ERP and about 51% on average for CMP, with Bjøntegaard Delta Encoding Time (BDET) gains approaching –50% and wall-clock speedups of up to 4.2×.

CCS CONCEPTS

- Information systems → Multimedia streaming.

KEYWORDS

360-degree Video, Fast Multirate Encoding, HEVC, Cubemap Projection, Adaptive Streaming

ACM Reference Format:

Amritha Premkumar, Christian Herglotz. 2026. Fast Multirate Encoding for 360° Video in OMAF Streaming Workflows. In *Mile-High Video Conference (MHV '26), February 02–05, 2026, Denver, CO, USA*. ACM, New York, NY, USA, 7 pages. <https://doi.org/10.1145/3789239.3793270>

1 INTRODUCTION

Immersive media is central to virtual reality (VR), augmented reality (AR), telepresence, education, and interactive entertainment. A common format is 360° video, which captures the full spherical environment and enables users to explore scenes with three rotational degrees of freedom [1, 2]. Delivering such content at high perceptual quality is challenging, as it demands ultra-high resolutions (4K–8K and beyond), high frame rates (60–120 fps), and specialized projection formats, imposing substantial computational and bandwidth burdens across capture, projection, compression, and streaming [3–6].

Modern immersive streaming relies on HTTP Adaptive Streaming (HAS) methods such as MPEG-DASH and HLS [7, 8], where each video is encoded into a bitrate ladder comprising multiple representations at different resolutions, bitrates, and QPs [9–11]. Clients switch among these representations to maintain uninterrupted playback. For 360° content, adaptivity is often paired with viewport-dependent or tile-based delivery so only the user's field of view is streamed at high quality [12–16]. Prior work spans viewport prediction, saliency, bitrate allocation, energy efficiency, and reinforcement learning-based adaptation [6, 15, 17–23], but most approaches assume that full multirate representation sets are already available, overlooking the substantial cost of preparing the underlying multirate representations—a gap our work explicitly targets [24] and which prior 360° HAS studies do not address.

This challenge is acute in OMAF workflows [25], which define projection metadata, viewport-adaptive signaling, and region-based mechanisms such as tiling or cubemap decomposition [12, 26, 27]. These features improve delivery efficiency but require many encoded bitstreams across resolutions and regions. Encoding 15 representations of an 8K 360° video can exceed 30 CPU-hours on commodity hardware [28], making exhaustive full-search encoding impractical for large VR libraries or latency-sensitive scenarios such as live streaming [29]. Recent work has further highlighted the importance of encoding latency and energy consumption as first-class optimization objectives in adaptive video streaming workflows [24]. Figure 1 illustrates this computational cost: encoding times rise sharply with resolution, while WSPSNR gains saturate unless bitrate increases significantly. Preparing a full ladder therefore requires repeated, expensive encodes, motivating fast multirate encoding techniques.

Fast multirate and multiresolution encoding exploits a key observation: encoder decisions are highly correlated across representations of the same content. Prior work [4, 5, 31] shows that CTU partitioning, intra/inter mode choices, motion estimation, and transform decisions remain structurally stable across QPs and resolutions. Reusing analysis from previously encoded representations can therefore avoid many redundant searches, substantially

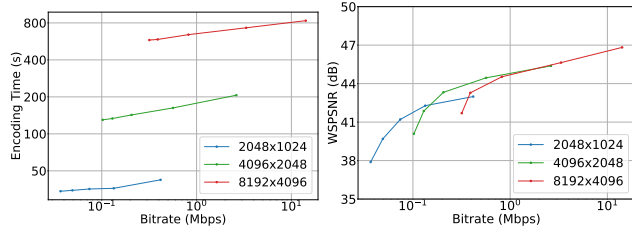


Figure 1: Rate-quality, and rate-encoding time curves of *Kaixuanmenye pano* [30]. Here, quality is represented using WSP-SNR.

reducing encoding time with modest RD impact [32, 33]. While x265 exposes analysis-reuse primitives [10, 34], their behavior for 360° layouts, OMAF-driven bitrate ladders, and cross-resolution pipelines has not been characterized; our work provides the first projection-aware evaluation of reuse flows.

Applying such reuse to spherical video, however, is challenging. Equirectangular projection (ERP), the dominant 360° layout, introduces strong geometric distortions near the poles [35, 36], affecting spatial and motion statistics and weakening cross-resolution consistency. Rotational motion, parallax, and viewport dynamics further increase temporal variability [26, 37]. Cubemap projection (CMP) offers a more uniform alternative: it decomposes the sphere into six square faces (Fig. 2), reducing geometric distortion and yielding more homogeneous block statistics [13, 38]. CMP also aligns naturally with OMAF’s region-based design, enabling independent, parallel face-wise encoding and amplifying the benefits of analysis reuse.

This work makes the following key contributions:

- (1) *Projection-Aware Multirate Encoding for 360° Video*: We extend multirate and multiresolution analysis-reuse methods to spherical video, addressing ERP distortions and viewport-driven variability, and show that CMP improves cross-resolution reuse stability.
- (2) *Comprehensive Evaluation on 8K 360° Content*: Using the SJTU 8K 360° dataset [30], we quantify encoding-time reductions, RD trade-offs, and scalability of the proposed techniques in OMAF-compliant pipelines, demonstrating substantial speedups with minimal RD loss.

Paper Outline: Section 2 reviews related work. Section 3 describes the proposed architecture, Section 4 details the experimental setup, Section 5 presents the results, and Section 6 concludes with future directions.

2 FAST MULTIRATE ENCODING

Generating full bitrate ladders for HAS is computationally expensive, especially for modern codecs like *High Efficiency Video Coding* (HEVC) and *Versatile Video Coding* (VVC) [39–41]. Fast multirate encoding addresses this by reusing encoder decisions—CTU partitioning, prediction modes, motion vectors, and transform choices—across representations of the same video, exploiting their strong correlation across QPs and resolutions [10, 32, 42]. This reuse can cut encoding time dramatically with minimal rate-distortion (RD) loss. Two main paradigms exist: *top-down* and *bottom-up*.

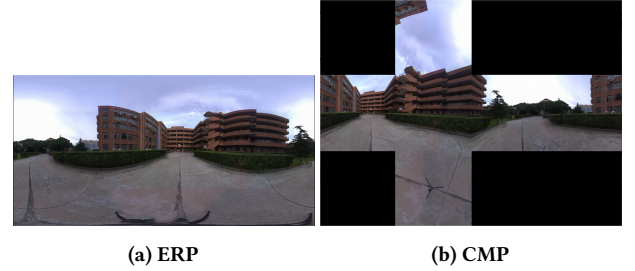


Figure 2: Comparison of 360° Projection Formats: ERP versus CMP.

2.1 Top-Down vs. Bottom-Up Paradigms

The *top-down* approach propagates decisions from the highest-quality representation (lowest QP or highest resolution) to others [32, 42]. While RD performance is strong, serialization limits parallelism, making it unsuitable for time-sensitive or large-scale workflows. Conversely, the *bottom-up* approach starts from the fastest-to-encode representation (lowest resolution or highest QP) [10, 33, 43]. Analysis becomes available early, enabling high concurrency and scalability. Although RD loss is slightly higher than top-down, bottom-up approaches are far more practical for VR/360° pipelines requiring dozens of representations.

2.2 Cross-Resolution and Cross-QP Prediction

Encoder analysis transfers well across neighboring QPs and resolutions. Cross-QP reuse exploits stable block-partitioning patterns, while cross-resolution reuse leverages spatial self-similarity [33, 42]. Mapping decisions across resolutions, however, requires precise scaling of CTU coordinates and block sizes. Recent heuristics and lightweight ML models improve robustness, but ultra-high-resolution encoding (4K–8K) still incurs significant complexity, motivating further optimization.

2.3 Challenges for 360° Video

Spherical video complicates reuse due to nonuniform pixel density. ERP, the dominant layout, introduces severe polar distortion, altering spatial and motion statistics and reducing transfer reliability. Consequently, existing multirate methods degrade when applied to 360° content. CMP mitigates these issues by decomposing the sphere into six square faces with uniform characteristics. CMP improves motion estimation, stabilizes block statistics, and enables independent face-wise encoding, unlocking massive parallelism. For OMAF-style pipelines requiring dozens of representations, these properties make CMP essential for practical, fast multirate encoding.

Without projection-aware acceleration, preparing full bitrate ladders for 8K 360° video remains prohibitively slow, motivating software-based fast multirate pipelines; hardware encoders offer high throughput but generally lack CTU-level analysis export/import, and therefore cannot participate in cross-QP or cross-resolution reuse. Our method addresses this gap by combining CMP with efficient cross-resolution and cross-QP reuse, delivering scalability without sacrificing RD performance.

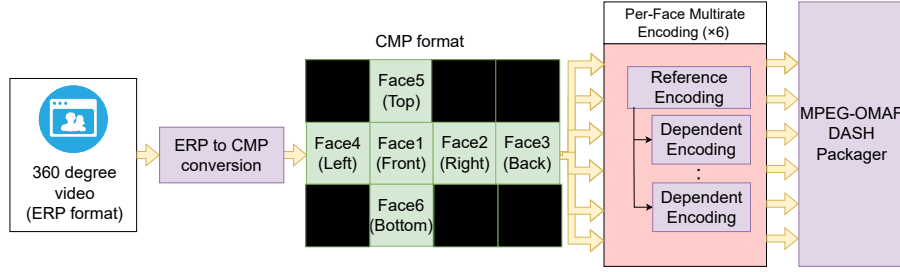


Figure 3: Overview of the proposed fast multirate encoding pipeline. The optional ERP→CMP conversion is applied only in CMP-CRC and CMP-PRA. For ERP-CRC and ERP-PRA, the pipeline omits the projection box; the multirate reuse logic (anchor + dependents, analysis save/load) remains identical.

3 PROPOSED FRAMEWORK

Our framework takes an input 360° ERP video and either (i) encodes it directly, or (ii) converts it to a CMP layout to reduce projection distortion and expose additional parallelism. We then perform fast multirate encoding by fully encoding a chosen *anchor* and reusing its analysis to accelerate the remaining *dependent* encodes. All resulting bitstreams are finally packaged into an OMAF-compliant DASH presentation (Figure 3).

We evaluate four practical variants by combining the projection format (ERP or CMP) with the analysis-sharing strategy (CRC or PRA):

- **ERP-CRC** : ERP projection with a cascaded HD→4K→8K flow.
- **ERP-PRA** : ERP projection with per-resolution anchors.
- **CMP-CRC** : CMP projection with a cascaded flow applied per face.
- **CMP-PRA** : CMP projection with per-face, per-resolution anchors.

ERP variants operate on a single full-frame tile, while CMP variants reuse analysis independently per face, unlocking more parallelism and benefiting from CMP's more uniform sampling.

At each resolution layer (HD, 4K, 8K), we select one *anchor* representation—low (LQ), medium (MQ), or high (HQ) quality—to run full RDO. Its decisions are reused to accelerate all *dependent* representations at the same resolution and, in CRC, at higher resolutions.

3.1 Spherical-to-Cubemap Projection

Formulation. Let the 360° content be defined on the sphere \mathbb{S}^2 by a radiance function

$$\mathcal{V} : \mathbb{S}^2 \times \mathbb{N} \rightarrow \mathbb{R}^3, \quad \mathcal{V}(\omega, t) = (Y, Cb, Cr), \quad (1)$$

where ω is a viewing direction and (Y, Cb, Cr) are YCbCr components. The ERP projection samples this function via

$$E(u, v, t) = \mathcal{V}(\omega_{\text{ERP}}(u, v), t), \quad (u, v) \in [0, W) \times [0, H). \quad (2)$$

The CMP layout maps \mathbb{S}^2 to six square domains Ω_k via

$$F_k(x, y, t) = \mathcal{V}(\omega_k(x, y), t), \quad (x, y) \in \Omega_k, \quad (3)$$

with $\omega_k(\cdot)$ denoting the face-specific inverse projection. CMP reduces geometric distortion and stabilizes encoder statistics, improving the reliability of cross-resolution reuse.

3.2 Rate Ladder and Representation Structure

Intuition. We encode a compact set of quality levels (CRFs) per face. Only the anchor performs full RDO; dependents reuse its analysis to skip most partitioning, mode, and motion searches.

Formulation. For each face k , the CRF ladder is

$$Q = \{q_0, q_1, \dots, q_{L-1}\}, \quad q_0 < q_1 < \dots < q_{L-1}, \quad (4)$$

with q_0 denoting the highest-quality anchor. Representation ℓ is encoded as

$$R_{k,\ell} = \mathcal{E}(F_k; q_\ell), \quad \ell \in \{0, \dots, L-1\}, \quad (5)$$

where $\mathcal{E}(\cdot)$ denotes x265 encoding with analysis saving/loading. Dependents load and reuse the anchor's analysis to accelerate encoding.

3.3 Reference Encoding: Full RDO and Analysis Extraction

The anchor at each resolution (or face) performs full RDO, exhaustively searching block partitions, prediction modes, and motion vectors. Optimal decisions are stored per frame and CU:

$$d_{k,0}^{(n,i)} = (s_{k,0}^{(n,i)}, m_{k,0}^{(n,i)}, v_{k,0}^{(n,i)}), \quad (6)$$

where s is the split pattern, m the prediction mode, and v the motion vector.

3.4 Dependent Encodings via Analysis Reuse

Overview. Dependent encodes reuse the anchor's decisions as strong priors, reducing the search space and avoiding expensive evaluations.

Formulation. For each $\ell \geq 1$:

$$d_{k,\ell} = \arg \min_{d \in S_{k,0}} (D(d) + \lambda(q_\ell) R(d)), \quad (7)$$

where admissible decisions satisfy:

- **Split reuse:** $s_{k,\ell}^{(n,i)} \preceq s_{k,0}^{(n,i)}$ (no deeper splits).
- **Mode reuse:** $m_{k,\ell}^{(n,i)} = m_{k,0}^{(n,i)}$ (skip mode search).
- **MV reuse:** $v_{k,\ell}^{(n,i)} = v_{k,0}^{(n,i)}$ (perform only local refinement).

For cross-resolution reuse (HD→4K, 4K→8K), x265 scales the anchor's analysis to the target CU grid.

Table 1: Framework variants combining projection and analysis-sharing strategy.

Variant	Projection	Strategy (flow)
ERP-CRC	ERP (single tile)	Cascaded HD→4K→8K
ERP-PRA	ERP (single tile)	Per-resolution anchors (HD, 4K, 8K)
CMP-CRC	CMP (6 faces)	Cascaded HD→4K→8K per face
CMP-PRA	CMP (6 faces)	Per-resolution anchors per face

3.5 Analysis Sharing Schemes: CRC and PRA

We compare two practical multiresolution strategies:

- **CRC:** A strict bottom-up cascade (HD→4K→8K). Each resolution has a single anchor whose analysis accelerates all dependents and seeds the next resolution. This maximizes cross-resolution reuse at minimal memory cost.
- **PRA:** Each resolution independently selects an anchor (LQ/MQ/HQ). Dependents reuse this anchor, and anchors assist in initializing the next resolution. PRA offers greater flexibility but stores one analysis file per resolution.

3.6 OMAF Packaging and Output

Encoded ERP or CMP representations are packaged into an OMAF-compliant DASH presentation, including projection metadata, region signalling, and representation descriptors, enabling seamless integration into standard viewport-adaptive players.

ERP suffers from distortion that weakens analysis reuse, and naïve full-search encoding of all ladder levels is prohibitively slow for 8K 360° content. By combining CMP’s uniformity and face-wise parallelism with CRC /PRA analysis sharing and per-resolution anchors (LQ/MQ/HQ), the framework achieves scalable multirate encoding with minimal RD loss and OMAF-ready outputs.

4 EXPERIMENTAL SETUP

4.1 Implementation Configuration in x265

Our framework builds on x265’s analysis–reuse subsystem [34, 43]. During each anchor encode, per-frame analysis is stored using *analysis-save*, and is later imported by dependent encodes via *analysis-load*. Reuse strength is controlled through *analysis-save-reuse-level* and *analysis-load-reuse-level*; we use the strongest setting (*level 10*), which preserves CU-level structure, prediction modes, and motion information.

Cross-QP reuse (same resolution). Dependent encodes reuse CU splits, inter modes, and motion information with *load-reuse-level=10*. Limited refinement is permitted using *refine-intra=4*, *refine-inter=2*, and *refine-mv=1*, ensuring robustness without sacrificing speed.

Cross-resolution reuse. For HD→4K and 4K→8K transitions, x265 scales CTU-level decisions using *scale-factor=2* together with level-10 reuse, eliminating most partitioning, mode search, and motion estimation at higher resolutions.

4.2 Dataset

We use the SJTU 360° dataset [30], which contains 15 ERP sequences at 8192 × 4096 resolution. The clips span 30 s each; in our setup, a single 8K full-search reference encode requires several minutes per

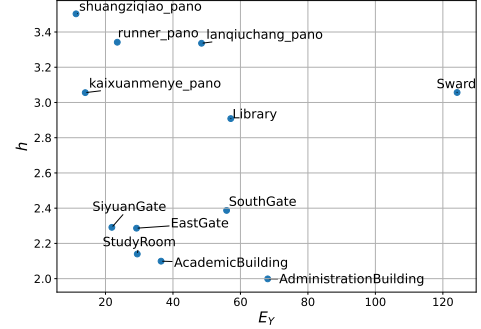


Figure 4: Complexity analysis of the SJTU dataset using (E_Y, h) from VCA [44]. Higher values indicate more complex motion and texture.

Table 2: Experimental parameters and values.

Parameter	Values
\mathcal{R}	{ 2048x1024 (HD), 4096x2048 (4K), 8192x4096 (8K) }
Q	{ 22, 27, 32, 37, 42 }
Target encoder	x265 [medium][intra period=1 s][4 CPU threads]
Target decoder	HM [1 CPU thread]

CRF, underscoring the cost of preparing full bitrate ladders. The distribution of content complexity, computed via (E_Y, h) features from the Video Complexity Analyzer (VCA) [44], is shown in Figure 4.

For projection-aware analysis and improved parallelism, each ERP sequence is converted to CMP using a standard sphere-to-cubemap mapping. This produces six uniformly sampled faces of size 2048 × 2048 corresponding to the {front, back, left, right, top, bottom}. Each face is treated as an independent tile during encoding.

All experiments are executed on a server with an Intel Xeon processor (32 threads) and 128 GB RAM, enabling both serial runtime evaluation (per tile) and parallel runtime evaluation (six tiles concurrently). Table 2 summarizes resolutions, QPs, and codec settings.

4.3 Metrics

All evaluations compare each proposed method against *ERP-Default*, the full-search ERP encode.

Quality metrics We compute PSNR and WSPSNR for each QP using Samsung 360tool.¹ Figure 5 illustrates the evaluation pipeline.

Serial encoding runtime difference (ΔT_S) Assuming sequential encoding, the relative runtime change is

$$\Delta T_S = \frac{\sum \tau_{\text{method}} - \sum \tau_{\text{ref}}}{\sum \tau_{\text{ref}}}. \quad (8)$$

Parallel encoding runtime difference (ΔT_P) Assuming concurrent encoding, runtime is dominated by the slowest representation:

$$\Delta T_P = \frac{\max(\tau_{\text{method}}) - \max(\tau_{\text{ref}})}{\max(\tau_{\text{ref}})}. \quad (9)$$

¹<https://github.com/Samsung/360tools>

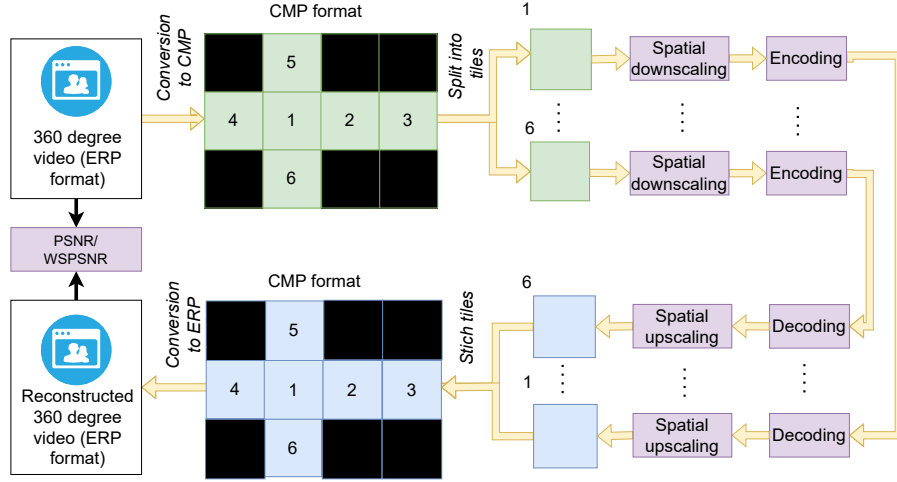


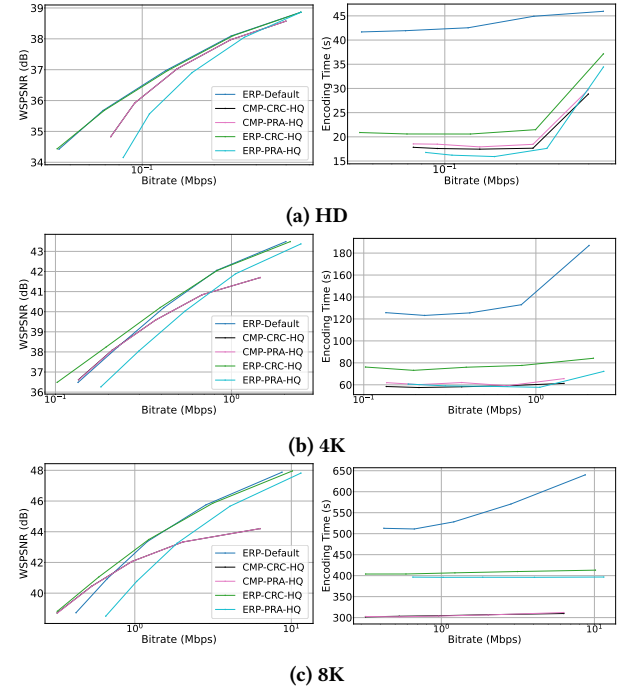
Figure 5: Quality evaluation framework.

Bjøntegaard Delta Metrics BD-PSNR and BD-WPSNR measure average quality differences relative to ERP-Default [45], where positive values denote gains and negative values small losses. BDET [46] evaluates relative encoding-time savings at equal quality; negative BDET indicates faster encoding for the same RD performance.

5 RESULTS AND DISCUSSION

Encoding-Speed Gains. Figure 6 compares WPSNR and encoding time across HD, 4K, and 8K for the *Academic Building* sequence. The left plots show rate-WPSNR curves, while the right plots show encoding time versus bitrate. ERP-Default yields the highest encoding times at all resolutions, reflecting the cost of exhaustive full-search encoding. Both CRC and PRA provide substantial speedups, with PRA showing the most aggressive reductions. CMP-based variants (CMP-CRC and CMP-PRA) amplify these gains through face-wise parallelism, offering the greatest benefits at 8K where ERP-Default exceeds 600 s per representation. In terms of quality, CRC follows ERP-Default most closely, whereas PRA deviates slightly—capturing the fundamental trade-off between speed and RD fidelity. At 4K, PRA provides the largest improvements, and CMP variants deliver the strongest overall throughput, highlighting the advantage of projection-aware reuse.

Table 3 summarizes performance relative to ERP-Default. For ERP content, CRC reduces serial time by 33 %–52 % and parallel time by 24 %–57 %. CMP-CRC further improves these numbers, reaching 50.82 % (serial) and 48.67 % (parallel). PRA achieves the largest raw reductions—45 %–47 % on average and up to 59 % at 4K—while CMP-PRA delivers the highest overall throughput, with average gains of 51.38 % (serial) and 49.88 % (parallel). These trends demonstrate that bottom-up reuse remains highly effective even under the more complex statistics of spherical video. Such savings are particularly valuable in production pipelines where dozens of representations must be prepared per sequence.

Figure 6: Rate-WPSNR and rate-encoding time curves for *Academic Building* at HD, 4K, and 8K.

Rate-Distortion Impact: CRC offers the most stable RD behavior, with ERP BD-PSNR/BD-WPSNR differences close to zero. CMP-CRC exhibits larger losses (up to -1.07 dB BD-PSNR), and PRA yields more pronounced deviations due to its more aggressive reuse granularity. However, WPSNR accounts for spherical sampling nonuniformity, and hence, it more closely reflects perceptual differences than planar PSNR in 360° content. Thus, the largest CMP-CRC drop at 8K appears primarily in planar PSNR; corresponding WPSNR

Table 3: Comparison of rate-distortion and encoding time savings for proposed methods relative to the ERP-Default encoding.

Method	Ref	Res	BD-PSNR [dB]	BD-WSPSNR [dB]	BDET (PSNR) [%]	BDET (WS-PSNR) [%]	ΔT_S [%]	ΔT_P [%]
ERP-CRC	LQ	HD	-0.06 ± 0.03	-0.06 ± 0.03	-47.09 ± 4.89	-47.07 ± 4.89	-43.63 ± 5.36	-24.20 ± 5.76
		4K	0.09 ± 0.06	0.08 ± 0.06	-50.43 ± 1.68	-50.43 ± 1.66	-51.57 ± 1.20	-56.64 ± 4.24
		8K	0.02 ± 0.13	-0.02 ± 0.14	-29.63 ± 5.22	-29.67 ± 5.20	-31.04 ± 5.45	-40.84 ± 5.87
		Avg	0.02 ± 0.07	0.00 ± 0.08	-42.38 ± 3.93	-42.39 ± 3.92	-42.08 ± 4.01	-40.56 ± 5.29
	MQ	HD	-0.01 ± 0.02	-0.01 ± 0.02	-41.47 ± 4.00	-41.44 ± 3.99	-42.86 ± 4.30	-23.56 ± 3.80
		4K	0.12 ± 0.06	0.10 ± 0.06	-48.29 ± 2.09	-48.28 ± 2.10	-49.45 ± 2.64	-54.32 ± 4.81
		8K	0.03 ± 0.12	0.00 ± 0.14	-29.43 ± 5.44	-29.47 ± 5.42	-30.86 ± 5.61	-40.85 ± 5.88
		Avg	0.05 ± 0.07	0.03 ± 0.07	-39.73 ± 3.84	-39.73 ± 3.84	-41.06 ± 4.18	-39.58 ± 4.83
	HQ	HD	-0.05 ± 0.05	-0.05 ± 0.06	-40.30 ± 5.92	-40.28 ± 5.92	-33.33 ± 7.06	0.18 ± 11.62
		4K	0.13 ± 0.04	0.12 ± 0.03	-44.29 ± 2.69	-44.28 ± 2.69	-45.57 ± 2.97	-50.41 ± 7.06
		8K	0.06 ± 0.09	0.03 ± 0.10	-27.76 ± 3.93	-27.80 ± 3.90	-29.22 ± 4.46	-38.55 ± 4.85
		Avg	0.05 ± 0.06	0.03 ± 0.06	-37.45 ± 4.18	-37.45 ± 4.17	-36.04 ± 4.83	-29.59 ± 7.84
ERP-PRA	LQ	HD	-0.19 ± 0.14	-0.18 ± 0.11	-54.28 ± 4.69	-54.25 ± 4.73	-50.62 ± 4.86	-25.00 ± 5.22
		4K	-0.26 ± 0.15	-0.26 ± 0.14	-55.99 ± 2.00	-56.10 ± 1.97	-59.06 ± 0.79	-63.61 ± 3.59
		8K	-0.44 ± 0.19	-0.41 ± 0.23	-27.02 ± 3.63	-27.21 ± 3.68	-32.35 ± 5.18	-42.62 ± 5.57
		Avg	-0.30 ± 0.16	-0.28 ± 0.16	-45.77 ± 3.44	-45.86 ± 3.46	-47.34 ± 3.61	-43.74 ± 4.79
	MQ	HD	-0.16 ± 0.03	-0.15 ± 0.03	-47.29 ± 5.52	-47.25 ± 5.49	-48.62 ± 5.16	-19.46 ± 6.89
		4K	-0.21 ± 0.08	-0.22 ± 0.07	-55.97 ± 1.42	-56.03 ± 1.38	-58.78 ± 1.15	-64.31 ± 3.36
		8K	-0.45 ± 0.20	-0.48 ± 0.23	-29.49 ± 4.35	-29.67 ± 4.36	-32.39 ± 5.17	-42.71 ± 5.50
		Avg	-0.27 ± 0.10	-0.29 ± 0.11	-44.25 ± 3.76	-44.31 ± 3.74	-46.59 ± 3.83	-42.16 ± 5.25
	HQ	HD	-0.54 ± 0.08	-0.55 ± 0.10	-54.39 ± 4.14	-54.34 ± 4.14	-46.86 ± 5.66	-11.03 ± 11.02
		4K	-0.76 ± 0.14	-0.79 ± 0.14	-55.91 ± 1.65	-55.92 ± 1.65	-56.66 ± 1.67	-58.37 ± 5.78
		8K	-1.18 ± 0.37	-1.26 ± 0.42	-30.49 ± 4.51	-30.56 ± 4.48	-31.89 ± 4.69	-41.13 ± 5.13
		Avg	-0.83 ± 0.20	-0.87 ± 0.22	-46.93 ± 3.43	-46.94 ± 3.42	-45.14 ± 4.01	-36.84 ± 7.31
CMP-CRC	HQ	HD	-0.60 ± 0.31	-0.29 ± 0.43	-49.56 ± 6.03	-50.24 ± 5.72	-46.33 ± 6.54	-27.66 ± 7.25
		4K	-0.92 ± 0.08	-0.56 ± 0.19	-54.92 ± 1.84	-55.11 ± 1.98	-58.01 ± 1.81	-62.96 ± 4.87
		8K	-1.70 ± 0.88	-1.44 ± 0.77	-43.77 ± 4.23	-43.99 ± 4.17	-48.12 ± 4.23	-55.40 ± 4.51
		Avg	-1.07 ± 0.42	-0.76 ± 0.46	-49.42 ± 4.04	-49.78 ± 3.96	-50.82 ± 4.19	-48.67 ± 5.54
CMP-PRA	HQ	HD	-0.60 ± 0.31	-0.29 ± 0.43	-50.41 ± 4.24	-51.05 ± 4.00	-47.59 ± 4.46	-30.76 ± 4.22
		4K	-0.94 ± 0.07	-0.57 ± 0.18	-55.24 ± 2.79	-55.40 ± 2.90	-58.28 ± 1.90	-63.46 ± 4.20
		8K	-1.70 ± 0.89	-1.45 ± 0.77	-43.98 ± 4.14	-44.19 ± 4.09	-48.27 ± 4.17	-55.43 ± 4.54
		Avg	-1.08 ± 0.42	-0.77 ± 0.46	-49.88 ± 3.73	-50.22 ± 3.66	-51.38 ± 3.51	-49.88 ± 4.32

differences are considerably smaller and remain visually acceptable for typical VR viewports, where spherical distortion patterns and user-centric masking reduce perceptibility.

Complexity and Resource Considerations: For N resolutions, CRC stores analysis ($N-1$) times, whereas PRA stores N anchors. Thus, CRC is somewhat more memory-efficient, though PRA's footprint remains manageable for modern servers. The comparison underscores a practical trade-off: CRC favors conservative reuse and compact resource use, while PRA sacrifices small amounts of RD precision for maximum throughput.

CMP-Based Variants and Practical Implications: CMP-CRC and CMP-PRA follow the ERP trends but benefit from independent face-wise processing, enabling the highest overall speedups (up to 4.2x). The additional parallelism, combined with more uniform face statistics, makes CMP-based pipelines particularly attractive for time-sensitive applications such as live VR streaming or rapid multi-representation preparation in large content libraries. These results, to our knowledge, constitute the first systematic comparison of analysis-reuse behavior under ERP and CMP projections within OMAF-compliant multirate encoding pipelines.

6 CONCLUSIONS AND FUTURE WORK

This paper presented a fast multirate encoding framework for cubemap 360° video in OMAF-compliant streaming workflows. Building on x265's analysis-reuse capabilities, we introduced two cross-resolution strategies—Cascaded Resolution Chain (CRC) and

Per-Resolution Anchoring (PRA)—along with their cubemap-based counterparts, CMP-CRC and CMP-PRA. Using the SJTU 8K 360° dataset, our experiments demonstrated that all variants achieve substantial encoding-time reductions compared to exhaustive full-search encoding, with BDET of up to -50 % and wall-clock speedups reaching 4.2x in the most favorable CMP-CRC configurations. Our results highlight a clear trade-off: CRC offers better RD fidelity and lower memory footprint (analysis stored $N-1$ times), while PRA maximizes encoding speed at the cost of modest RD degradation and slightly higher memory overhead (N anchors). Our CMP-based designs further exploit face-wise independence to enable parallel encoding, delivering up to 4.2x speedups and making the framework suitable for near-real-time scenarios such as live VR streaming. Importantly, these enhancements integrate seamlessly with OMAF's region-based architecture and DASH delivery without requiring client-side modifications.

Future work includes extending the proposed framework to VVC-based pipelines, exploring content-aware anchor selection and reuse strength (e.g., via machine learning or online complexity classification), and integrating viewport prediction or QoE-driven bitrate ladder optimization. Another promising direction is to combine the proposed encoder-side acceleration with decoder-side enhancements, such as super-resolution or view-adaptive upsampling, to enable next-generation immersive streaming services.

REFERENCES

- [1] A. Yaqoob, T. Bi, and G.-M. Muntean, "A survey on adaptive 360° video streaming: Solutions, challenges and opportunities," vol. 22, no. 4, pp. 2801–2838.
- [2] M. Zink, R. Sitaraman, and K. Nahrstedt, "Scalable 360° Video Stream Delivery: Challenges, Solutions, and Opportunities," vol. 107, no. 4, pp. 639–650.
- [3] K.-C. Huang, P.-Y. Chien, C.-A. Chien, H.-C. Chang, and J.-I. Guo, "A 360-degree panoramic video system design," in *Technical Papers of 2014 International Symposium on VLSI Design, Automation and Test*, pp. 1–4.
- [4] Y. He, X. Xiu, P. Hanhart, Y. Ye, F. Duanmu, and Y. Wang, "Content-Adaptive 360-Degree Video Coding Using Hybrid Cubemap Projection," in *2018 Picture Coding Symposium (PCS)*, pp. 313–317, ISSN: 2472-7822.
- [5] J. Carreira, S. M. M. de Faria, L. M. N. Tavora, A. Navarro, and P. A. Assuncao, "Versatile Video Coding Of 360° Video Using Adaptive Resolution Change," in *2020 IEEE International Conference on Image Processing (ICIP)*, pp. 3398–3402, ISSN: 2381-8549.
- [6] X. Chen and G. Cao, "Energy-Efficient 360-Degree Video Streaming on Multicore-Based Mobile Devices," in *IEEE INFOCOM 2023 - IEEE Conference on Computer Communications*, pp. 1–10, ISSN: 2641-9874.
- [7] I. Sodagar, "The MPEG-DASH Standard for Multimedia Streaming Over the Internet," in *IEEE MultiMedia*, vol. 18, no. 4, 2011, pp. 62–67.
- [8] R. Pantos and W. May, "HTTP Live Streaming," RFC 8216, 2017. [Online]. Available: <https://rfc-editor.org/rfc/rfc8216.txt>
- [9] A. Bentaleb, B. Taani, A. C. Begen, C. Timmerer, and R. Zimmermann, "A Survey on Bitrate Adaptation Schemes for Streaming Media Over HTTP," *IEEE Communications Surveys & Tutorials*, vol. 21, no. 1, pp. 562–585, 2019.
- [10] V. V. Menon, H. Amirpour, M. Ghanbari, and C. Timmerer, "EMES: Efficient Multi-encoding Schemes for HEVC-based Adaptive Bitrate Streaming," *ACM Trans. Multimedia Comput. Commun. Appl.*, vol. 19, no. 3s, Mar. 2023.
- [11] V. V. Menon, P. T. Rajendran, C. Feldmann, K. Schoeffmann, M. Ghanbari, and C. Timmerer, "JND-Aware Two-Pass Per-Title Encoding Scheme for Adaptive Live Streaming," *IEEE Transactions on Circuits and Systems for Video Technology*, vol. 34, no. 2, pp. 1281–1294, Feb. 2024.
- [12] D. Monakhov, I. D. Curcio, and S. Mate, "On data wastage in viewport-dependent streaming," in *2019 IEEE 21st International Workshop on Multimedia Signal Processing (MMSP)*, pp. 1–6, ISSN: 2473-3628.
- [13] Y. Shinohara, S. Shirasaki, Y. Wu, K. Kanai, and J. Katto, "Performance evaluations of tile-based 360-degree DASH streaming with clustering-based viewport prediction," in *2019 IEEE International Conference on Consumer Electronics - Taiwan (ICCE-TW)*, pp. 1–2.
- [14] A. Yaqoob and G.-M. Muntean, "A combined field-of-view prediction-assisted viewport adaptive delivery scheme for 360° videos," vol. 67, no. 3, pp. 746–760.
- [15] S.-Z. Qian, Y. Zhang, and T. Lin, "FBRA360: A fuzzy-based bitrate adaptation scheme for 360° video streaming," in *2023 IEEE International Conference on Multimedia and Expo Workshops (ICMEW)*, pp. 122–127.
- [16] M. Tang and V. W. Wong, "Online bitrate selection for viewport adaptive 360-degree video streaming," vol. 21, no. 7, pp. 2506–2517.
- [17] W. Feng, S. Wang, and Y. Dai, "Adaptive 360-degree streaming: Optimizing with multi-window and stochastic viewport prediction," vol. 24, no. 7, pp. 5903–5915.
- [18] Q. Yang, W. Gao, C. Li, H. Wang, W. Dai, J. Zou, H. Xiong, and P. Frossard, "360Spred: Saliency Prediction for 360-Degree Videos Based on 3D Separable Graph Convolutional Networks," vol. 34, no. 10, pp. 9979–9996.
- [19] I. U. Khan, K. Han, and J. W. Lee, "TransUser's: A Transformer Based Salient Object Detection for Users Experience Generation in 360° Videos," in *2024 IEEE International Conference on Artificial Intelligence and eXtended and Virtual Reality (AIxVR)*, pp. 256–260.
- [20] M. Orduna, P. Pérez, J. Gutiérrez, and N. García, "Content-immersive Subjective Quality Assessment in Long Duration 360-degree Videos," in *2023 15th International Conference on Quality of Multimedia Experience (QoMEX)*, pp. 73–78.
- [21] J. Tu, C. Chen, Z. Yang, M. Li, Q. Xu, and X. Guan, "PSTile: Perception-Sensitivity-Based 360° Tiled Video Streaming for Industrial Surveillance," vol. 19, no. 9, pp. 9777–9789.
- [22] Z. Jiang, X. Zhang, Y. Xu, Z. Ma, J. Sun, and Y. Zhang, "Reinforcement Learning Based Rate Adaptation for 360-Degree Video Streaming," vol. 67, no. 2, pp. 409–423.
- [23] A. Katsenou, V. V. Menon, G. Laurinaviciute, B. Bross, and D. Marpe, "Multi-Objective Pareto-Front Optimization for Efficient Adaptive VVC Streaming," 2026. [Online]. Available: <https://arxiv.org/abs/2601.10607>
- [24] V. V. Menon, A. Premkumar, P. T. Rajendran, A. Wieckowski, B. Bross, C. Timmerer, and D. Marpe, "Energy-efficient Adaptive Video Streaming with Latency-Aware Dynamic Resolution Encoding," in *Proceedings of the 3rd Mile-High Video Conference*, ser. MHV '24, 2024, p. 21–27.
- [25] M. M. Hannuksela and Y.-K. Wang, "An Overview of Omnidirectional MediA Format (OMAF)," *Proceedings of the IEEE*, vol. 109, no. 9, pp. 1590–1606, 2021.
- [26] C. Cortés, P. Pérez, J. Gutiérrez, and N. García, "Influence of Video Delay on Quality, Presence, and Sickness in Viewport Adaptive Immersive Streaming," in *2020 Twelfth International Conference on Quality of Multimedia Experience (QoMEX)*, pp. 1–4.
- [27] M. Yang, W. Zou, J. Song, and F. Yang, "Enhancing QoE for Viewport-Adaptive 360-Degree Video Streaming: Perception Analysis and Implementation," vol. 28, no. 4, pp. 64–73.
- [28] J. Kufa, L. Polak, M. Simka, and A. Stech, "Software and Hardware Encoding of Omnidirectional 8K Video: A Performance Study," in *2023 33rd International Conference Radioelektronika (Radioelektronika)*, pp. 1–5.
- [29] S. Singh and J. Chakareski, "Aerial 360-Degree Video Delivery for Immersive First Person View UAV Navigation," in *2023 IEEE International Symposium on Multimedia (ISM)*, pp. 139–146.
- [30] X. Liu, Y. Huang, L. Song, R. Xie, and X. Yang, "The SJTU UHD 360-Degree Immersive Video Sequence Dataset," in *2017 International Conference on Virtual Reality and Visualization (ICVRV)*, pp. 400–401, ISSN: 2375-141X.
- [31] D. Wang, S. Du, Y. Sun, S. Xia, F. Dufaux, H. Guo, G. Wang, and C. Zhu, "Fast CU Partition Algorithm For 360-Degree Videos on VVC," in *2025 IEEE International Conference on Multimedia and Expo (ICME)*, pp. 1–6, ISSN: 1945-788X.
- [32] D. Schroeder, P. Rehm, and E. Steinbach, "Block structure reuse for multi-rate high efficiency video coding," in *2015 IEEE International Conference on Image Processing (ICIP)*, 2015, pp. 3972–3976.
- [33] V. V. Menon, A. Wieckowski, Y. Liu, B. Bross, and D. Marpe, "Block-Partitioning Strategies for Accelerated Multi-rate Encoding in Adaptive VVC Streaming," 2025. [Online]. Available: <https://arxiv.org/abs/2510.14645>
- [34] A. Matheswaran, P. K. Karadugattu, P. Ramachandran, A. Giladi, D. Grois, P. Venkatesan, and A. Balk, "Open source framework for reduced-complexity multi-rate HEVC encoding," in *Applications of Digital Image Processing XLIII*, A. G. Tescher and T. Ebrahimi, Eds., vol. 11510, International Society for Optics and Photonics. SPIE, 2020, p. 115101Y.
- [35] B. Ray, J. Jung, and M.-C. Larabi, "A Low-Complexity Video Encoder for Equirectangular Projected 360 Video Content," in *2018 IEEE International Conference on Acoustics, Speech and Signal Processing (ICASSP)*, 2018, pp. 1723–1727.
- [36] Y. He, Y. Ye, P. Hanhart, and X. Xiu, "Geometry Padding for Motion Compensated Prediction in 360 Video Coding," in *2017 Data Compression Conference (DCC)*, pp. 443–443, ISSN: 2375-0359.
- [37] D. V. Nguyen, H. T. T. Tran, and T. C. Thang, "Impact of delays on 360-degree video communications," in *2017 TRON Symposium (TRONSHOW)*, pp. 1–6.
- [38] K. K. Sreedhar, A. Aminlou, M. M. Hannuksela, and M. Gabbouj, "Viewport-Adaptive Encoding and Streaming of 360-Degree Video for Virtual Reality Applications," in *2016 IEEE International Symposium on Multimedia (ISM)*, pp. 583–586.
- [39] G. J. Sullivan, J.-R. Ohm, W.-J. Han, and T. Wiegand, "Overview of the high efficiency video coding (HEVC) standard," in *IEEE Transactions on circuits and systems for video technology*, vol. 22, no. 12. IEEE, Dec. 2012, pp. 1649–1668.
- [40] B. Bross, Y.-K. Wang, Y. Ye, S. Liu, J. Chen, G. J. Sullivan, and J.-R. Ohm, "Overview of the Versatile Video Coding (VVC) Standard and its Applications," vol. 31, no. 10, 2021, pp. 3736–3764.
- [41] I. Siqueira, G. Correia, and M. Grellert, "Rate-Distortion and Complexity Comparison of HEVC and VVC Video Encoders," in *IEEE 11th Latin American Symposium on Circuits & Systems (LASCAS)*, 2020.
- [42] D. Schroeder, A. Ilangoan, and E. Steinbach, "Multi-rate encoding for HEVC-based adaptive HTTP streaming with multiple resolutions," in *2015 IEEE 17th International Workshop on Multimedia Signal Processing (MMSP)*, 2015, pp. 1–6.
- [43] K. Goswami, B. Hariharan, P. Ramachandran, A. Giladi, D. Grois, K. Sampath, A. Matheswaran, A. K. Mishra, and K. Pikus, "Adaptive Multi-Resolution Encoding for ABR Streaming," in *2018 25th IEEE International Conference on Image Processing (ICIP)*, 2018, pp. 1008–1012.
- [44] V. V. Menon, C. Feldmann, K. Schoeffmann, M. Ghanbari, and C. Timmerer, "Green Video Complexity Analysis for Efficient Encoding in Adaptive Video Streaming," in *Proceedings of the First International Workshop on Green Multimedia Systems*, 2023, p. 16–18.
- [45] HSTP-VID-WPOM, "Working Practices Using Objective Metrics for Evaluation of Video Coding Efficiency Experiments," *International Telecommunication Union*, 2020. [Online]. Available: <http://handle.itu.int/11.1002/pub/8160e8da-en>
- [46] C. Herglotz, A. Heindel, and A. Kaup, "Decoding-Energy-Rate-Distortion Optimization for Video Coding," in *IEEE Transactions on Circuits and Systems for Video Technology*, vol. 29, no. 1, Jan. 2019, p. 171–182.